Earthquakes and Structures, *Vol. 12, No. 2 (2017) 237-250*
DOI: https://doi.org/10.12989/eas.2017.12.2.237

External retrofit of beam-column joints in old fashioned RC structures

Mahdi Adibi*, Mohammad S. Marefat[a], Kamyar Karbasi Arani and Hamid Zare

School of Civil Engineering, College of Engineering, University of Tehran, Iran

(Received June 4, 2016, Revised January 9, 2017, Accepted January 13, 2017)

Abstract. There has been increasing attention in many countries on seismic retrofit of old fashioned RC structures in recent years. In such buildings, the joints lack transverse reinforcement and suffer inadequate seismic dimensional requirements and the reinforcement is plain bar. The behavior of the joints is governed by sliding of steel bars and diagonal shear failure is less influential. Different methods to retrofit beam-column joints have been proposed in the literature such as wrapping the joint by FRP sheets, enlargement of the beam-column joint, and strengthening the joint by steel sheets. In this study, an enlargement technique that uses external prestressed cross ties with steel angles is examined. The technique has already been used for substructures reinforced by deformed bars and has advantages such as efficient enhancement of seismic capacity and lack of damage to the joint. Three reference specimens and two retrofitted units are tested under increasing lateral cyclic load in combination with two levels of axial load. The reference specimens showed relatively low shear strength of $0.15\sqrt{(f_c)}$ and $0.30\sqrt{(f_c)}$ for the exterior and interior joints, respectively. In addition, relatively brittle behavior was observed and large deformations extended into the panel zone of the joints. The retrofit method has increased ductility ratio of the interior beam-column joints by 63%, and energy dissipation capacity by 77%, relative to the control specimen; For external joints, these values were 11%, and 94%. The retrofit method has successfully relocated the plastic joints far from the column face. The retrofit method has improved shear strength of the joints by less than 10%.

Keywords: seismic retrofit; old fashioned RC structures; exterior and interior beam-column joints; plain bars, steel angles prestressed by cross ties

1. Introduction

There has been increasing emphasis in many countries on seismic assessment and retrofit of existing reinforced concrete structures designed to the pre-1970's seismic codes in recent years (e.g., ATC 1989, Marthong *et al*. 2016, Park *et al*. 1995, Sazen *et al*. 2003-2000). This is a consequence of the observed severe damages to old buildings under moderate to great earthquakes in comparison with those designed to current design codes (ATC 1989). Among different elements, the beam-column joints have been highly susceptible to seismic excitations and the failure of joint panel has been frequently observed (e.g., ATC 1989, Hakuto *et al*. 1995, Park *et al*. 1995, Sazen *et al*. 2003-2000).

Experimental studies of concrete structures reinforced by deformed bars have shown that failure of the joint panels is governed either by shear mode or by deterioration of bond between steel and concrete. The stress distribution due to flexural and shear forces produce a wide diagonal crack pattern in the panel which leads to crush of the compressive strut, and consequently, to decline its strength and stiffness. The bond between concrete and steel also diminishes under cyclic action of the joint, and this in turn, yields to reduced flexural strength and ductility of the framing elements (Hakuto *et al*. 1999, Manfredi *et al*. 2008), and an increase in the story drift (Soleimani *et al*. 1979).

In absence of transverse reinforcement in the joint region, the post-cracking behavior depends solely on the efficiency of the compression strut mechanism to transfer the shear within the joint (Pampanin *et al*. 2006). The confinement in interior joints is more effective than exterior joints due to their geometry and presence of two beams at opposite sides. Thus, Interior joints are less vulnerable than exterior joints and exhibit a much more stable hysteretic behavior with hardening after first cracking (Calvi *et al*. 2002).

In concrete structures reinforced by plain bars the behavior of joints is different from those reinfeorced by deformed bars. That is, the mode of sliding of steel bars commonly governs failure of the joint and diagonal shear failure is less influential (Calvi *et al*. 2002, Liu and park 2000-2001, Bedirhanoglu *et al*. 2010, Russo and Pauletta 2012, Braga *et al*. 2009). Braga *et al*. (2012a, b) have presented a simplified steel bar model that incorporates the interaction between longitudinal bars and surrounding material. The model has made very convenient the computational procedure in the analytical simulations.

Different experimental studies (Pampanin *et al*. 2002, Calvi *et al*. 2002) on joints reinforced by plain bars have shown that low shear capacity of panel zone prevents formation of flexural plastic hinge in beams. In addition, early sliding of plain bars, especially in beams, prevents a beam to reach its ideal flexural capacity, and this prevents

*Corresponding author, Ph.D. Candidate
E-mail: m.adibi@ut.ac.ir
[a]Professor
E-mail: mmarefat@ut.ac.ir

ISSN: 2092-7614 (Print), 2092-7622 (Online)

shear cracking to form in the joint.

Different methods to retrofit beam-column joints have been proposed in the literature such as wrapping the joint by fiber reinforced polymer (FRP) sheets, enlargement of the beam-column joint, and strengthening the joint by steel sheets (Rohma *et al*. 2012, Marthong *et al*. 2016, Dimitrios and Tsonos 2010, Pimanmasa and Chaimahawan 2010, Karayannis *et al*. 2008). A number of these investigations in this area is reviewed subsequently.

Liu and Park (2001) tested four exterior beam-column joints reinforced by plain round bars subjected to simulated seismic loading. The column regions adjacent to the joint core were jacketed with fiber glass. The study shows that the retrofit technique improves stiffness and strength of the units greatly. In a study by Russo and Pauletta (2012), the longitudinal bars of the beam were anchored to steel plates placed on the exterior column surface. As a result, the strength of the beam-column joint increased and yielding of the beam bars produced higher dissipation of energy. Also Marthong *et al*. (2013) used epoxy resin infused under pressure into the damaged region for rehabilitation of beam-column joints and the rehabilitated connections exhibited equal or marginally better performance than before.

Shafaei *et al*. (2014a, b) suggested a retrofit method for concrete joints reinforced by deformed bars. In this method, the connection area was strengthened by steel angles prestressed by cross ties where stiffeners were welded to the angles (see Fig. 1). The proposed method showed significant enhancement of the seismic capacity of the joints, in terms of strength, stiffness, energy dissipation and ductility. Also the technique improved the bond between longitudinal reinforcement and concrete in the joint.

In this study, the technique proposed by Shafaei *et al*. (2014a, b) is extended to substructures reinforced by plain bars. The technique has some important advantages such as efficient enhancement of seismic capacity, relatively low cost, and lack of damage to the joint.

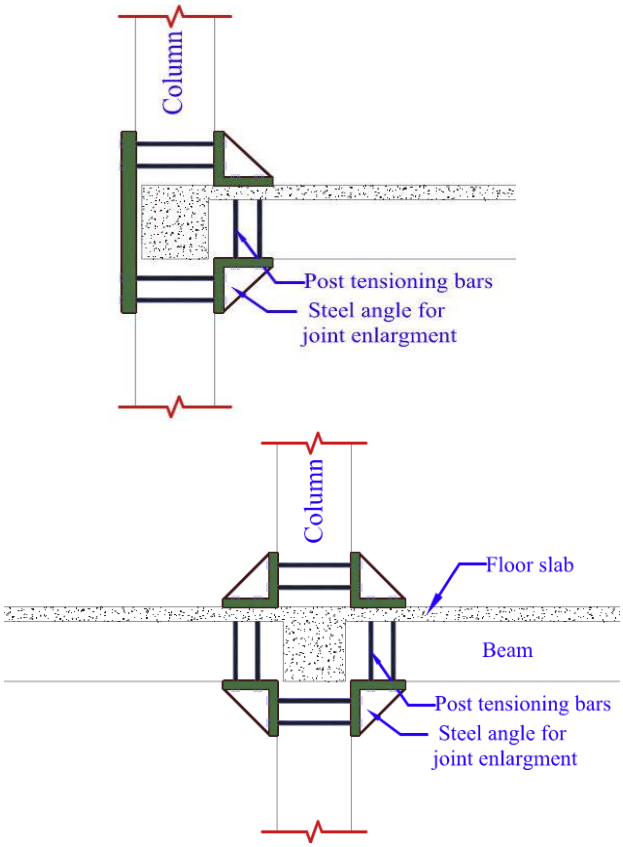

(a) Specifications of the proposed retrofit method

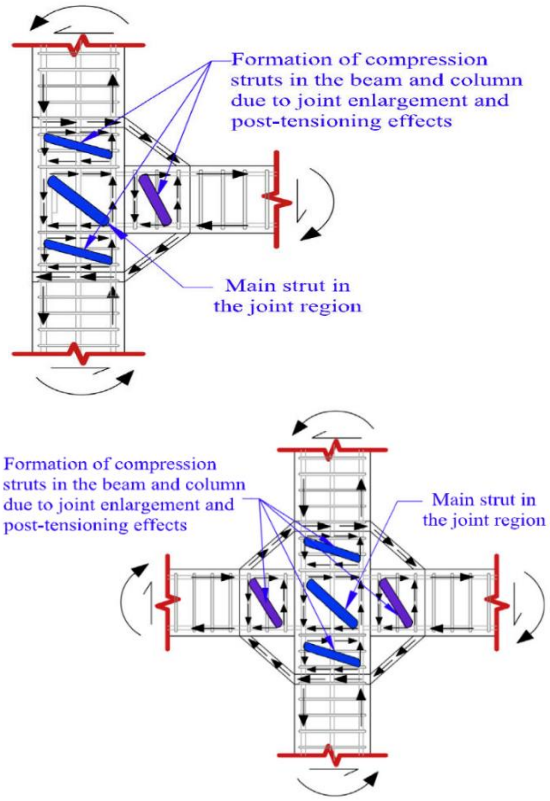

(b) Load transfer mechanisms in the joint before and after retrofitting

Fig. 1 Characteristics of the retrofit method for the joint (Shafaei *et al*. 2014a)

2. Joint shear force and shear resistance

Various models have been proposed by several researchers for predicting the RC beam-column joint shear strength. Most of these models were calibrated and verified with some limited experimental database (Parate and Kumar 2016).

Adjacent members transmit internal forces to the joint which results in joint shear forces in both horizontal and vertical directions, as shown in Fig. 2(a) (Paulay and Priestley 1992, Masi et al. 2009, Hakuto et al. 2000). These shear forces cause diagonal compression and tension stresses in the joint panel. Under increasing load, the latter will usually result in diagonal cracking of the concrete core and the mechanism of shear resistance changes drastically.

Basic mechanisms of shear transfer in the joint are shown in Fig. 2. Some of the internal forces will combine to develop a diagonal strut (see Fig. 2(b)). Other forces, transmitted to the joint core from beam and column bars by means of bond, produce a truss mechanism, as is shown in Fig. 2(b) (Paulay and Priestley 1992). As a result, both

horizontal and vertical shear reinforcement will be required to prevent shear failure by diagonal tension (see Fig. 2(b)). Such reinforcement will enable a diagonal compression field to be mobilized which provides a feasible load path for both horizontal and vertical shearing forces (Paulay and Priestley 1992).

According to Fig. 2(a), the horizontal shear force in the joint region is equal to (Masi *et al*. 2009)

$$V_{jh} = C_{s2} + C_{c2} + T_1 - V_c' \quad (1)$$

In addition, sectional equilibrium of the beams yields to (Masi *et al*. 2009)

$$C_{s2} + C_{c2} = T_2 \quad (2)$$

$$V_{jh} = C_{s2} + C_{c2} + T_1 - V_c' = T_2 + T_1 - V_c' \quad (3)$$

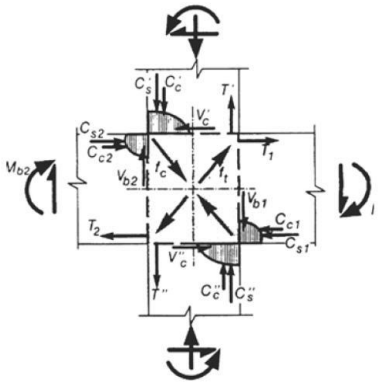

(a) Force acting on joint core

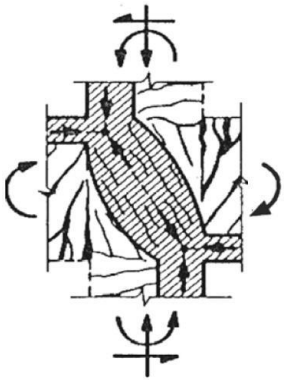

(b) Strut-mechanism

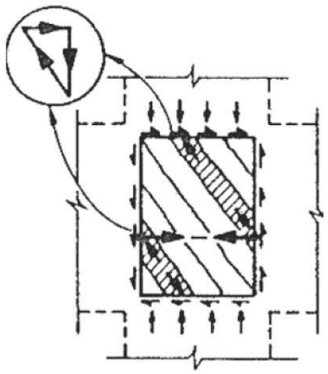

(c) Truss-mechanism

Fig. 2 Mechanisms of shear transfer at an interior beam-column joint (Paulay and Priestley 1992)

And for exterior beam-column joint (Masi *et al*. 2009)

$$V_{jh} = C_{s2} + C_{c2} - V_c' \quad (4)$$

$$C_{s2} + C_{c2} = T_2 \quad (5)$$

$$V_{jh} = T_2 - V_c' \quad (6)$$

The normal horizontal shear stress at the mid-depth of joint core can be written as

$$v_{jh} = V_{jh}/b_j h_c \quad (7)$$

Where, b_j is effective width of the joint core and h_c is depth of the column. NZS 3101:1995 defines b_j as either the smaller of

$$b_j = b_c \ \ or \ \ (b_w + 0.5h_c) \ \ when \ \ b_c \geq b_w \quad (8)$$

$$b_j = b_c \ \ or \ \ (b_c + 0.5h_c) \ \ when \ \ b_c \leq b_w \quad (9)$$

Where, b_c is width of the column and b_w is width of beam web.

It is important to note that deterioration of bond along the longitudinal bars does not change the total shear force acting on the joint (Hakuto *et al*. 2000).

In these old-fashioned joints, due to lack of hoops in the joint region, the joint shear is concentrated in a single compressed concrete strut (Calvi *et al*. 2002). The principal stresses in the joint panel (f_c and f_t) can be given by Mohr's Circle assuming uniform normal and transverse stresses, f_a and v_{jh}, respectively, according to the following equation (see Fig. 2) (Masi *et al*. 2009)

$$f_c = -\frac{f_a}{2} - \sqrt{(\frac{f_a}{2})^2 + {v_{jh}}^2} \quad (10)$$

$$f_t = -\frac{f_a}{2} + \sqrt{(\frac{f_a}{2})^2 + {v_{jh}}^2} \quad (11)$$

Calvi *et al*. (2002) suggested the value of $0.2\sqrt{f_c}$ for principal tensile stress at first cracking in the exterior joints reinforced by plain bars with end-hooks. It should be noted that the effect of axial load was not considered in the mentioned study.

3. Typical old fashioned RC structure

The interior and exterior beam–column joints are considered to be isolated from an existing three-story residential RC building built prior to the 1970s (Din-1045 1959, Duhman 1953, Pernot 1954, Guerrin 1959, Barker 1979, Edvard and Tanner 1996) and having an inter-story height of 2.9 meters and a beam effective span of 5.5 meters. Typical details of the reinforcement of the frame are shown in Figs. 3-4 and Table 1. The main defects of the nonseismic beam-column joints include use of plain bar, absence of transverse steel hoops, and the anchorage condition of longitudinal reinforcements. The anchorage length of the beam bars is almost equal to the joint effective width with 180-degree hooks at the ends of the bars. Also, these interior and exterior beam-column joints did not satisfy the requirements of "strong column and weak beam" principle.

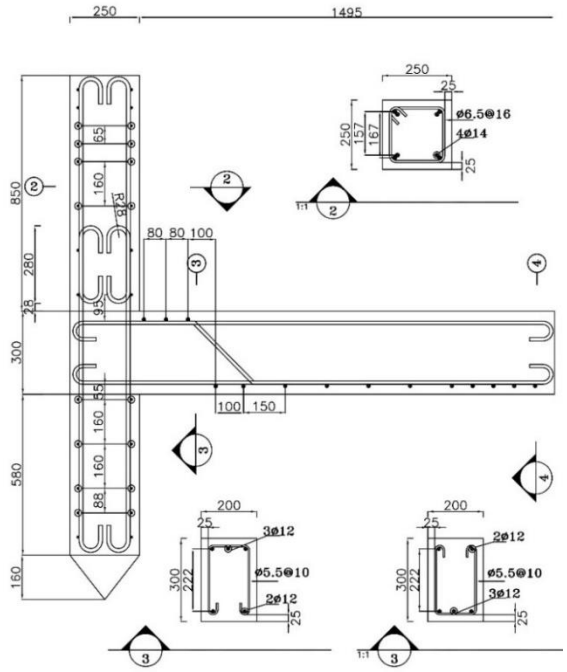

Fig. 3 Dimensions and reinforcement details of exterior beam-column joint of Specimen SC1

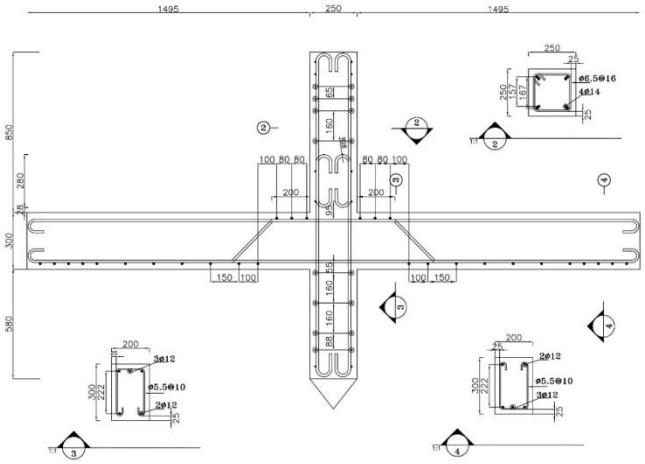

Fig. 4 Dimensions and reinforcement details of interior beam-column joint of Specimen SC2

The experimental program consisted of reverse-cyclic quasi-static unidirectional loading of five half scale exterior and interior RC beam-column joints. Three units (SC1, SC1-1 and SC2) were tested as-built to serve as control exterior and interior beam-column joints, and two units (SR3 and SR4) were seismically retrofitted prior to testing using adjustable scheme of joint enlargement for exterior and interior concrete beam-column joints. The nomenclature used for the various test specimens is presented in Table 1.

Dimensions and reinforcement of the beam and column in interior joints were identical to exterior joints (see Figs. 3-4). All of specimens except SC1-1 undergo axial loads to columns of 7% of section capacity ($A_g f'_c$), and the Specimen SC1-1 undergoes axial load to column of 15% of $A_g f'_c$.

The cross section dimensions of column and beam are

Table 1 Schedule of test specimens

Specimen	$P/A_g f'_c$	Objective	Loading	Col		Beam			Specification
				ρ_{col}	Av/s (mm)	ρ_{top}	ρ_{bot}	Av/s (mm)	
SC1	0.07	Control	Cyclic	0.01	0.396	0.0057	0.0038	0.32	Exterior joint
SC1-1	0.15	Control	Cyclic	0.01	0.396	0.0057	0.0038	0.32	Exterior joint
SC2	0.07	Control	Cyclic	0.01	0.396	0.0057	0.0038	0.32	Interior joint
SR3	0.07	Retrofit	Cyclic	0.01	0.396	0.0057	0.0038	0.32	Exterior joint
SR4	0.07	Retrofit	Cyclic	0.01	0.396	0.0057	0.0038	0.32	Interior joint

A_g: gross sectional area
f'_c: standard cylinder compressive strength of concrete
A_v: cross-sectional area of each stirrup
s: spacing of stirrups
ρ: longitudinal reinforcement ratio

Table 2 Compressive strength of concrete for different specimens

Specimen	Compressive Strength (MPa)
SC1	23.6
SC1-1	22.5
SC2	23.6
SR3	23.7
SR4	24.9

Table 3 Mechanical properties of reinforcement bars

Bar Diameter (mm)	Position	Yield Strength (MPa)	Ultimate Strength (MPa)	Yield Strain (ε_y)	Ultimate Strain (ε_{max})
5.5	Beam Stirrup	340	470	0.0012	0.28
6.5	Column Stirrup	224	336	0.0013	0.25
12	Beam Longitudinal Bar	360	500	0.0015	0.28
14	Column Longitudinal Bar	320	450	0.0017	0.30

ε_{max}: strain at which fracture occurs

250*250 mm and 200*300 mm, respectively. The column is reinforced by 4Φ14 plain bars, 1% reinforcement ratio, and the transverse reinforcement is Φ6.5 plain bars with 135 end hooks that are spaced at 160 mm outside the joint panel zone only. It was assumed that points of contraflexure would occur at the mid-height of columns and the mid-span of beams. The details of the control specimens are shown in Figs. 3-4.

Concrete strength of specimens at the age of testing and the mechanical properties of the steel reinforcement used in the specimens are shown in Tables 2-3.

4. Proposed retrofit method

The technique is based on prevention or delay of sliding of the smooth bars, as the governing mode of failure, and

Table 4 Characteristic of retrofitted specimens

Retrofitted specimen	Angle	Back plate	Number of cross bolts			Specification
			Along beam	Along column	Prestressing Value	
SR3	2L150×75 ×10	PL450×330 ×10	4	4	$0.5f_y$	Exterior joint
SR4	4L150×150 ×10	—	8	8	$0.5f_y$	Interior joint

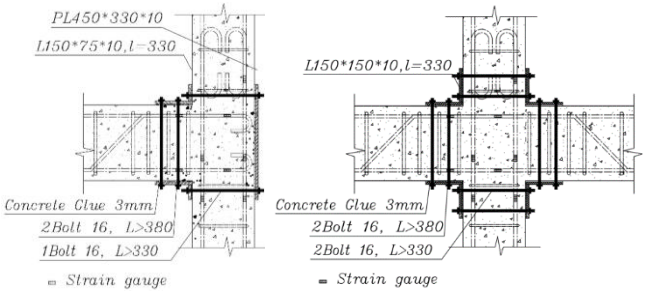

(a) Specimen SR3 (b) Specimen SR4

Fig. 5 Dimensions and reinforcement details of retrofitted specimens (dimensions in millimeters)

relocation of the large deformation zone to a distance away from the joint region. In terms of load transfer, the use of angles prestressed by cross-ties leads to two-dimensional enlargement of beam-column joints (see Fig. 1). In exterior and interior joints, steel angles are placed at all corners of the joints and linked to a steel plate or steel angles at the opposite side.

Specimens SR3, as an exterior beam-column joint was retrofitted by steel angles of 150 mm*75 mm*10 mm and a steel plate of 450 mm*330 mm*10 mm (see Fig. 5(a)). The crossing bolts in this specimen were prestressed by approximately 50% of f_y. The crossing bolts were high tensile strength M16 bars, used by washers and nuts. The length and specified ultimate tensile strength of the prestressed bars were 400 mm and 1000 MPa respectively. Tightening was achieved using a calibrated wrench and the tension in all bolts was checked by a repeat pass to ensure that all bolts were prestressed to the prescribed value.

The retrofit method used for Specimen SR3, was similar to Specimen SR4 as an interior beam-column joint (see Fig. 5(b)). The characteristics of retrofitted specimens are shown in Fig. 5 and Table 4. In all specimens, concrete adhesive was used between the angles and the joints.

5. Method of loading

The test setup is illustrated in Fig. 6. Lateral cyclic loading with increasing amplitudes is quasi-statically applied to the top of the column by a hydraulic actuator with a ±100 kN loading capacity and a ±200 mm displacement range. Also a vertical ±250 kN capacity hydraulic jack was used to apply constant axial load to the column by means of a link beam. For each specimen a total of 10 electrical resistance straingauges were attached to longitudinal and transverse reinforcement at critical locations, and 13 linear variable displacement transducers (LVDTs) were used to record the deformation of the beam

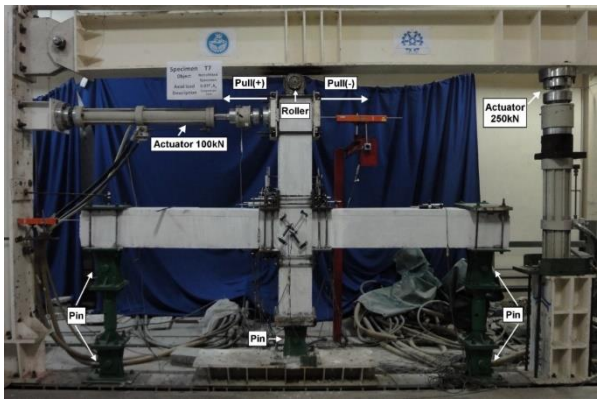

Fig. 6 Overview of test setup and instrumentation

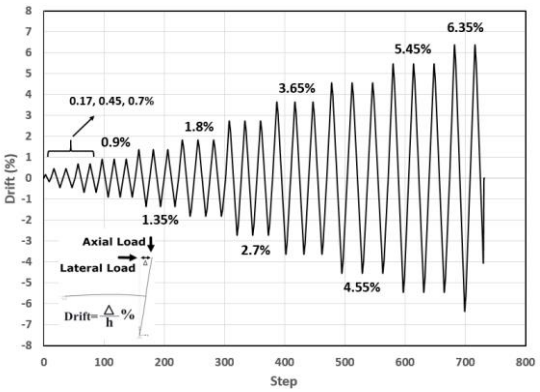

Fig. 7 Lateral cyclic loading protocol

and column and joint distortion, as shown in Fig. 6. Positive and negative loading directions and the hydraulic jacks are indicated in Fig. 6.

Two levels of axial load representing the story level were applied to the column: $0.07f'_c.b.h$, and $0.15f'_c.b.h$, where b and h are the width and depth of the cross section of the column and P is the axial load. The axial load was applied in a force controlled mode and was maintained constant throughout each test. Low rate lateral cyclic loading of increasing amplitudes was applied at the top of the column in a displacement controlled mode. The loading procedure for all specimens was based on ACI 374.2R-13 (2005) and ACI 374.1-05 (2005). Fig. 7 shows the lateral cyclic loading protocol.

6. Results and discussion

6.1 Exterior beam-column joint

6.1.1 Control Specimens SC1 and SC1-1

Fig. 8 illustrates development of flexural cracks of exterior joint, Specimen SC1, at different stages. The first cracks formed at a drift ratio of 0.45% at two locations of the beam: at a distance of 37 cm far from the column face and at the intersection of beam with column. After that, additional flexural cracks appeared over the zone where longitudinal bars were bent. During elastic behavior, the joint and the column did not undergo any cracking.

Beyond a drift ratio of 1.35%, the crack pattern did not

vary significantly, instead, rocking behavior governed the response and spalling of concrete cover at the joint region appeared. Width of intersectional crack at this drift ratio was approximately 10 mm. At a drift ratio of 1.8%, longitudinal cracks parallel to longitudinal bars developed over the beam. In addition, diagonal cracks in the joint panel zone commenced at this drift ratio.

The specimen has reached its nominal flexural strength (corresponding to 15.8 kN lateral force) in pull direction (the strength of weak face of the beam which controls bearing capacity of the substructure (see Table 5)). This was also confirmed by straingages that indicated strain values of ξ_y during the test.

In push direction (strong face of the beam), the specimen did not develop full nominal flexural strength and reached 17 kN lateral load that was only 0.73% of its nominal capacity (22.6 kN). The straingages on top longitudinal bars recorded a maximum strain of 0.80 ξ_y during the test. Overall, the smooth bars have prevented the beam to reach its full nominal sectional strength.

At a drift ratio of 2.7%, concrete wedge spalling at the exterior face of the joint was observed and at a drift ratio of 3.65%, X-shape cracks in the joint panel is formed and concrete wedge spalled and crushed off.

The relationship between drift and lateral force and the effect of P-Δ of Specimen SC1 are shown in Fig. 10(a). The curve shows relatively high pinching effect and relatively rapid decline of strength with increasing displacement. The pinching may be attributed primarily to sliding of the smooth bars and shear failure in the joint region while the rapid decline of strength is primarily caused by P-Δ effect as is shown in the Fig. 10(a). The large contribution of P-Δ effect may be described by the pattern of crack and damage to the specimen. That is, a few wide cracks have divided the beam into a few solid segments, and this has caused rocking fluctuation of the segments under cyclic action, and therefore, relatively large P-Δ effect.

The control Specimen SC1-1 underwent axial load to columns as much as 15% of the section capacity (Agf'c). The relationship between drift and lateral force and the effect of P-Δ of Specimen SC1-1 are shown in Fig. 10-b. The curve shows relatively high pinching effect and relatively more rapid decline of strength with increasing displacement compared to control Specimen SC1.

Table 5 Peak test load and ductility of positive and negative directions

Specimen	Peak load (kN) F_y			Drift at yield point ξ_y			Ultimate Drift ξ_u			Ductility factor μ		
	Pull (+)	Push (-)	Average	Pull (+)	Push (-)	Average	Pull (+)	Push (-)	Average	Pull (+)	Push (-)	Average
SC1	15.8	-17	16.4	0.49	-0.95	0.72	1.99	-4.67	3.33	4.08	4.937	4.51
SC1-1	23.8	-15.3	19.55	0.57	-0.58	0.57	1.35	-2.87	2.11	2.38	4.95	3.67
SC2	27.7	-22.5	25.1	1.47	-1.59	1.53	5.50	-6.20	5.85	3.73	3.90	3.82
SR3	12.6	-19.9	16.3	0.49	-0.59	0.54	2.30	-3.10	2.70	4.75	5.26	5.01
SR4	29.9	-30.2	30.1	0.87	-0.83	0.85	5.40	-5.20	5.3	6.18	6.30	6.24

δ_u: drift at either 20% drop of peak load, buckling of longitudinal reinforcement, fracturing of longitudinal or transverse reinforcement (whichever occurs first)

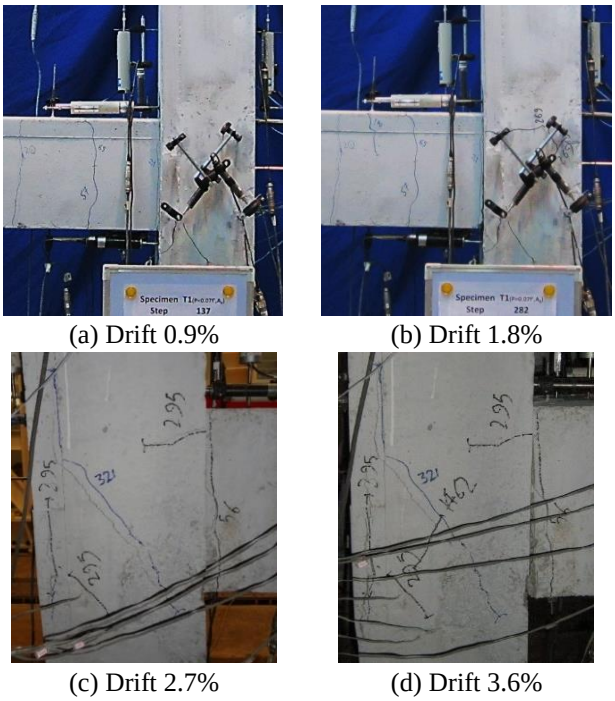

(a) Drift 0.9% (b) Drift 1.8%

(c) Drift 2.7% (d) Drift 3.6%

Fig. 8 Damage progression and crack observation for control Specimen SC1

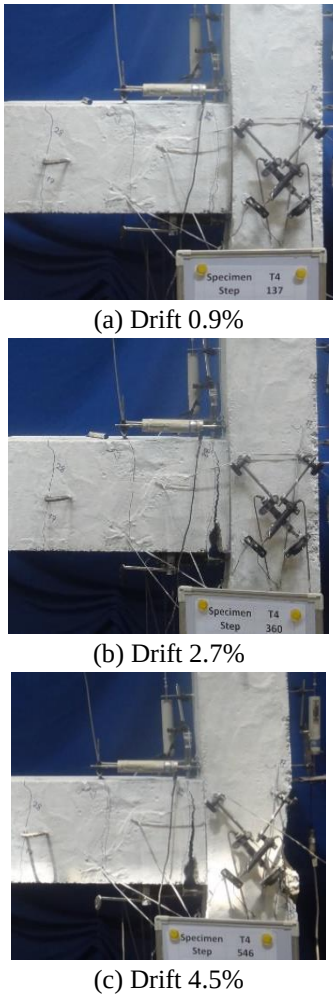

(a) Drift 0.9%

(b) Drift 2.7%

(c) Drift 4.5%

Fig. 9 Damage progression and crack observation for control Specimen SC1-1

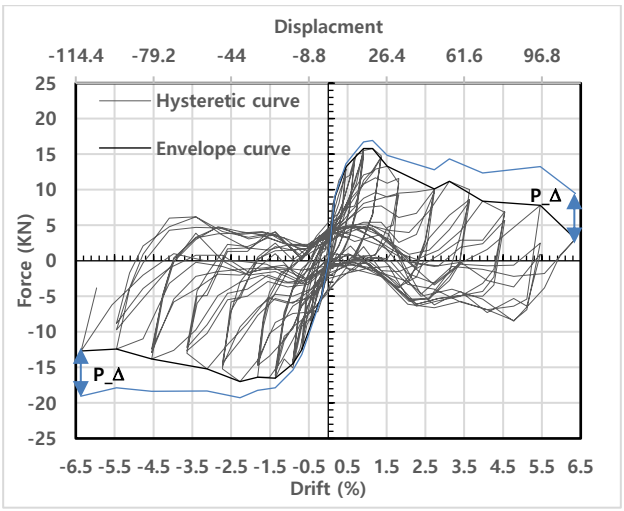

(a) Specimen SC1

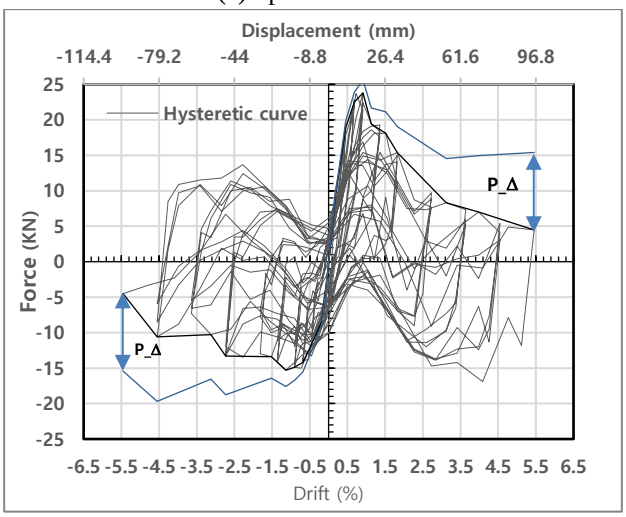

(b) Specimen SC1-1

Fig. 10 Hysteretic curve, P-Δ effect, and backbone curve of control Specimen SC1 and SC1-1

Axial load in this specimen was larger and caused larger contribution of P-Δ effect relative to Specimen SC1 (Fig. 10(b)). An increase of 50% of flexural strength in pull direction is seen in comparison with SC1. The strain-gages recorded 3200 μs on bottom longitudinal bars of the beam that indicates post yield strength of the bars. In push direction (strong face of the beam), the specimen did not develop full nominal flexural strength like Specimen SC1. Overall, larger axial force in the column has raised flexural strength of the joint by an average rate of 25%.

6.1.2 Retrofitted Specimen SR3

Specimen SR3 was retrofitted by a steel angle of 150 mm*75 mm*10 mm with a prestressing rate of 50% of f_y, as shown in Fig. 5.

Fig. 11 illustrates development of flexural cracks of specimen SR3 at different stages. The first cracks formed at a drift ratio of 0.45% at two locations of the beam: at a distance of 5 cm far from the angle and at the point that the top bar is bent downward at a distance of 35 cm far from the column face. After that, additional flexural cracks

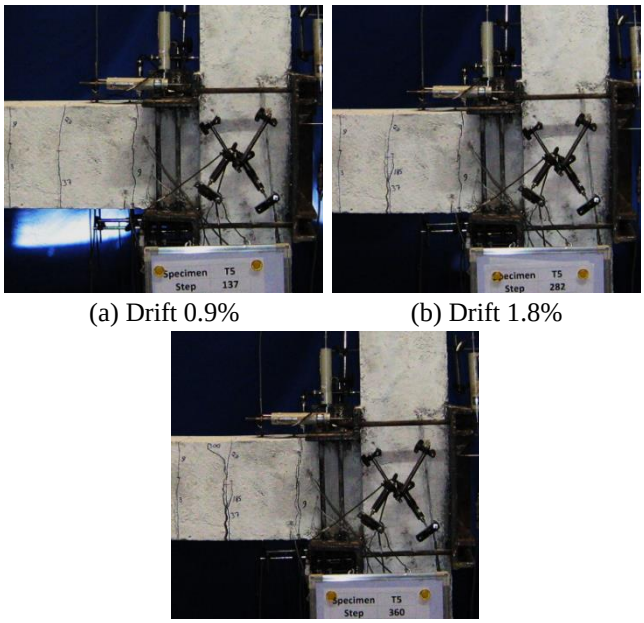

(a) Drift 0.9% (b) Drift 1.8%

(c) Drift 2.7%

Fig. 11 Damage progression and crack observation of retrofitted exterior joint Specimen SR3

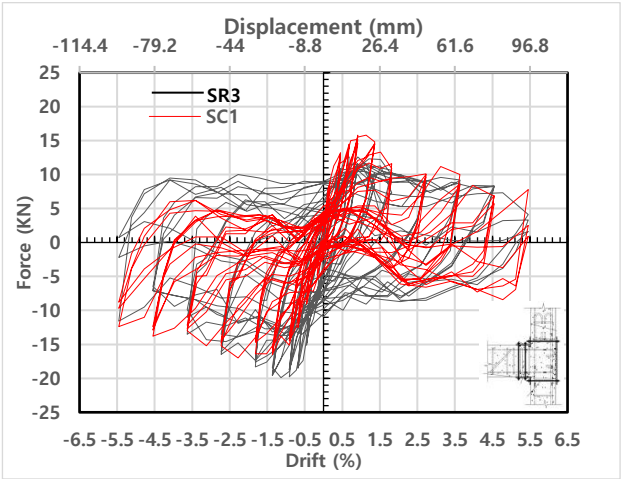

(a) Hysteresis curves

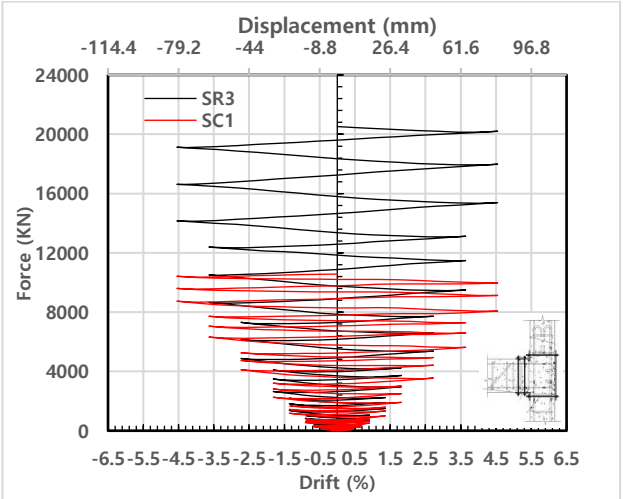

(b) Cumulative hysteresis energy dissipation curves

Fig. 12 Hysteresis and cumulative hysteresis energy dissipation curves of specimens SR3 and SC1

appeared over the beam.

At drift ratios larger than 1.35%, crack pattern did not vary and all of damage almost concentrated in two main cracks.

In comparison to control specimens, this specimen underwent cracks over longer length, and no diagonal cracks formed over the joint region.

The hysteresis curve of Specimen SR3 as an exterior beam-column joint is shown in Fig. 12(a), and it has been compared to the reference Specimen SC1. Fig. 12(a) indicates an increase of bearing capacity by 17% in push direction which is comparable to Specimen SC1. In pull direction, the bearing capacity has not been improved. But, the effect of pinching has been reduced significantly and the magnitude of hysteresis energy has been increased by almost twice. In addition, a more stable and ductile response is observed in comparison with SC1 (see Fig. 12).

6.2 Interior beam-column joint

6.2.1 Control Specimen SC2

Fig. 13 illustrates development of flexural cracks of interior joint Specimen SC2 at different stages. The first cracks formed at a drift ratio of 0.2% at the intersection of the beam with column in the left beam and at a distance of 11 cm far from the column face in the right beam.

Linear behavior of this specimen developed up to more drift ratio than SC1. Also flexural deformation in interior joint specimen developed over longer length and more drift ratio than the exterior joint specimen that exhibited a much more stable hysteretic behavior with hardening after first cracking.

At drift ratio of 1.35%, longitudinal cracks parallel to longitudinal bars developed over the beam in the joint region and spalling of concrete cover at the joint region appeared. Also width of intersectional crack in Specimen SC2 was 2 mm, while it was approximately 10 mm in Specimen SC1. It indicated that the slipping of the longitudinal bars of the beam in interior joint specimen was less than exterior joint specimen since they were continuous over the beam.

Like exterior beam-column joint, Specimen SC1, a few wide cracks dividing the substructure into a few solid elements was seen in this specimen and it indicated large contribution of P-Δ effect in behavior of substructure.

Hysteresis behavior of this specimen (see Fig. 14) is almost similar in both directions due to symmetric geometry and did not develop full nominal flexural strength and reached 25.1 kN average lateral load that was only 0.81% of its nominal capacity (31.1 kN). It seems that having continuous longitudinal bars in top and bottom of the beam without any hook caused bearing capacity of the substructure to fall down in comparison with exterior beam-column joint, Specimen SC1.

At drift ratio of 2.7%, first flexural cracks in the top column appeared whereas no crack in the column was observed during the test in exterior beam-column joint. Also the crack pattern over the beam did not vary significantly,

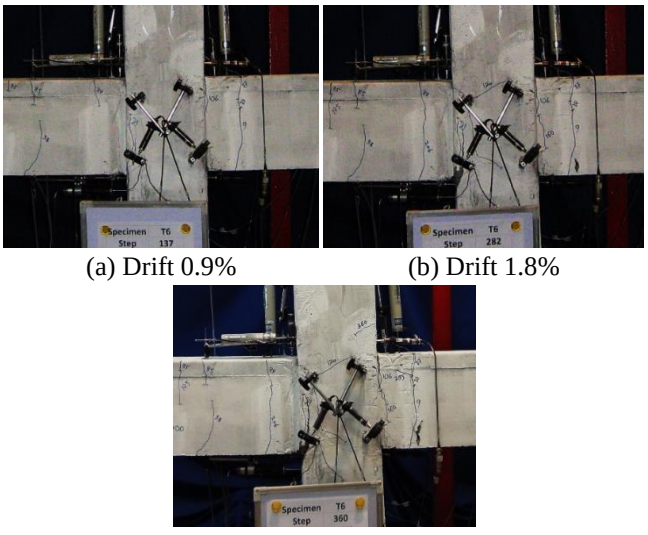

(a) Drift 0.9% (b) Drift 1.8%

(c) Drift 2.7%

Fig. 13 Damage progression and crack observation for control Specimen SC2

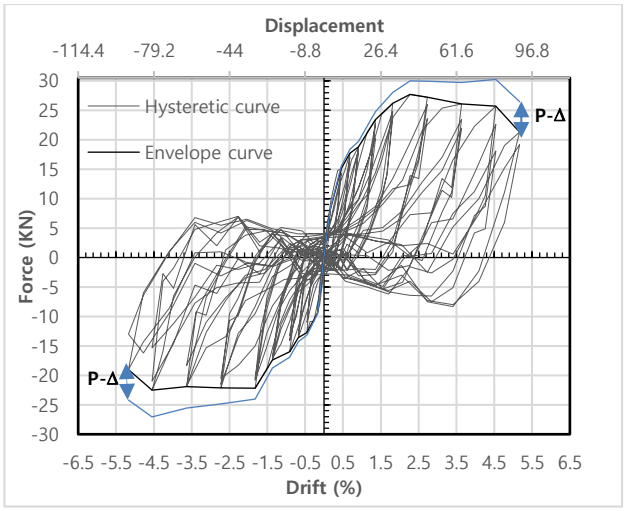

Fig. 14 Hysteretic curve, P-Δ effect, and backbone curve of control Specimen SC2

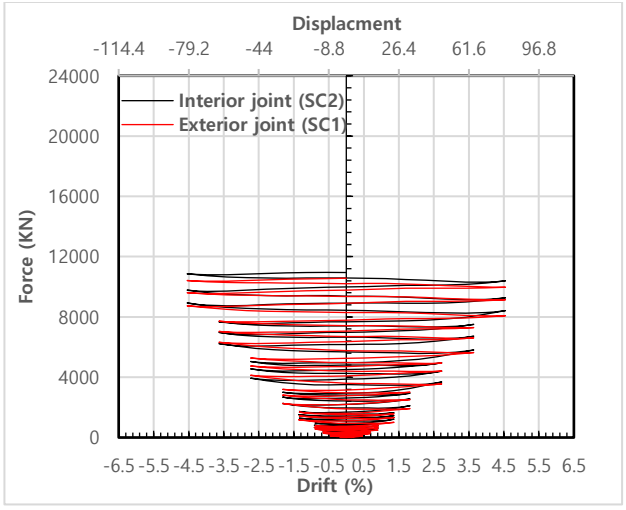

Fig. 15 Cumulative hysteresis energy dissipation curves for control Specimens SC1 and SC2

and instead, rocking behavior governed the response of substructure. Any diagonal cracks in the joint panel zone were not seen in this specimen. Also it was seen no serious damage to the column during loading, although being the beam stronger than column.

It was seen Low rate of strength deterioration with increasing displacement in hysteresis curve of this specimen in comparison with exterior beam-column joint that was attributed to the low sliding of the smooth bars and absence of any shear cracks in the joint region.

The cumulative energy dissipated from the beginning of the test till ±4.5% drift ratio for specimens SC1 and SC2 were 10.57 and 10.58 kN.m, respectively (see Fig.15). It is seen that interior beam-column joint displayed low rate of dissipation energy like the exterior beam-column joint.

6.2.2 Retrofitted Specimen SR4

Specimen SR4 as an interior beam-column joint was retrofitted by four steel angles of 150 mm*150 mm*10 mm at each corner of the joint, with a prestressing rate of 50% of f_y without any stiffener plates, as shown in Fig. 5(b).

As shown in Figs. 11 and 16, an almost regular and consistent pattern of cracks are observed in both retrofitted exterior and interior beam-column joints, that is, two relatively wide cracks are formed at 5 cm and at 20 cm next to the angle. The latter is located where the longitudinal bar at the top is bent to bottom face of the beam. In comparison to control Specimen, retrofitted specimens underwent cracks over longer length, and no diagonal cracks formed over the joint region.

As shown in Fig. 16, the first flexural cracks formed at a drift ratio of 0.2%. After that, additional flexural cracks appeared over the beam by increasing load.

The first flexural crack in the column appeared at top of the angle at a drift ratio of 0.9%, whereas in control Specimen SC2, flexural cracks in the column were seen at drift ratio of 2.7%. Also unlike other specimens, a flexural crack was seen in the bottom column at bottom of the angle,

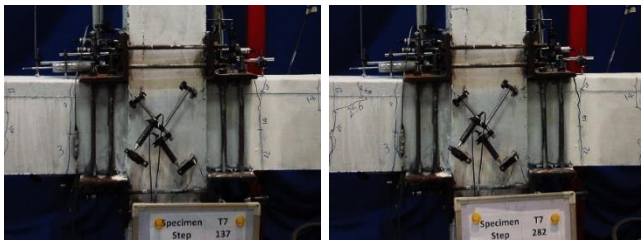

(a) Drift 0.9% (b) Drift 1.8%

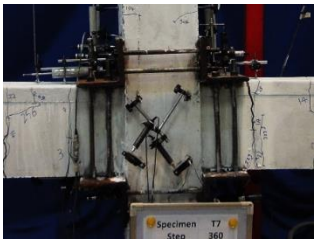

(c) Drift 2.7%

Fig. 16 Damage progression and crack observation for retrofitted Specimen SR4

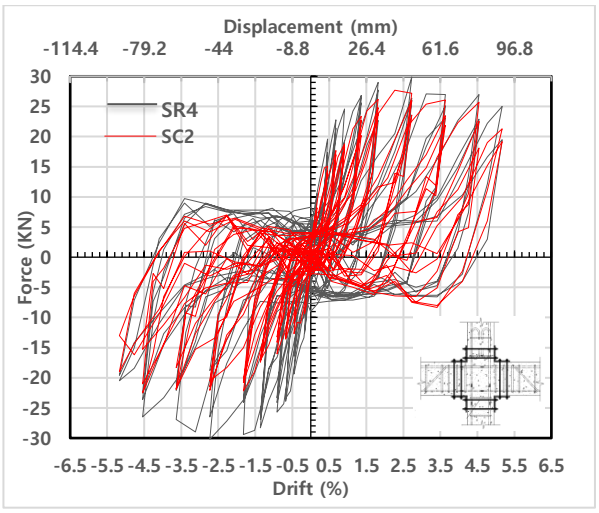

(a) Hysteresis curves

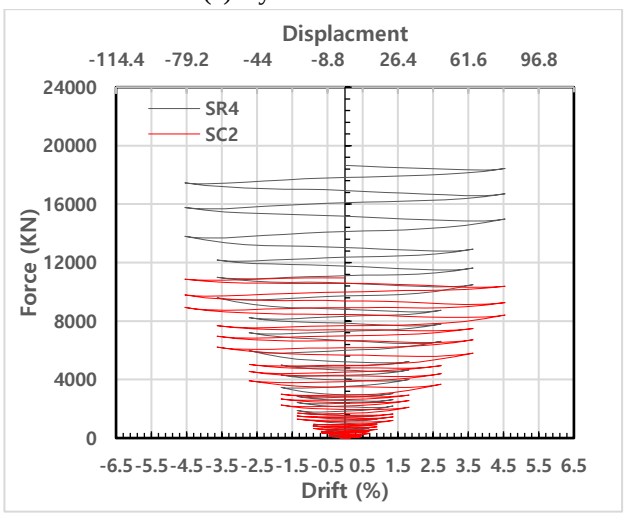

(b) Cumulative hysteresis energy dissipation curves

Fig. 17 Hysteresis and cumulative hysteresis energy dissipation curves of specimens SR4 and SC2

at drift ratio of 1.35%. After that, damage almost concentrated in two main cracks beside the angles in beams. Spalling of concrete cover beside the angle in beams is seen at drift ratio of 3.65%. No diagonal cracks in the joint panel zone and serious damage to the column were seen in this specimen.

The hysteresis curve of Specimen SR4 as an interior beam-column joint is shown in Fig. 17(a), and it has been compared to the reference Specimen SC2.

Using retrofit method caused bearing capacity of the specimen has been improved in both of directions. Average bearing capacity has been increased 20% in retrofitted Specimen SR4 in comparison with Specimen SC2.

The energy dissipated from the beginning of the test till ±4.5% drift ratio for retrofitted Specimen SR4 was 18.65 kN.m (see Fig. 17(b)). The effect of pinching has been reduced in the hysteresis curve and the magnitude of hysteresis energy has been increased almost 1.77 times in comparison with SC2. Using the retrofit method for exterior joint was more effective in dissipation of energy than interior joint.

Overall, the proposed retrofit method for exterior and interior beam-column joints seems satisfactory and effective, by relocating the wide crack away from the joint region, and by improving energy dissipation capacity and showing more stable and ductile behavior.

7. Force-displacement envelope curves

The envelope curves of all specimens based on peak force are shown in Figs. 18(a)-(b). The peak load, ultimate drifts and ductility capacity are reported in Table 5. The value of ductility is obtained from the idealized bilinear response (see Fig. 19) (Park 1989, Priestley and Park 1987). The ultimate drift, δ_u, is defined as the drift corresponding to either a 20% drop of peak load, the buckling of longitudinal reinforcement, fracturing of longitudinal or transverse reinforcement (whichever occurs first) (Paulay and Priestley 1992).

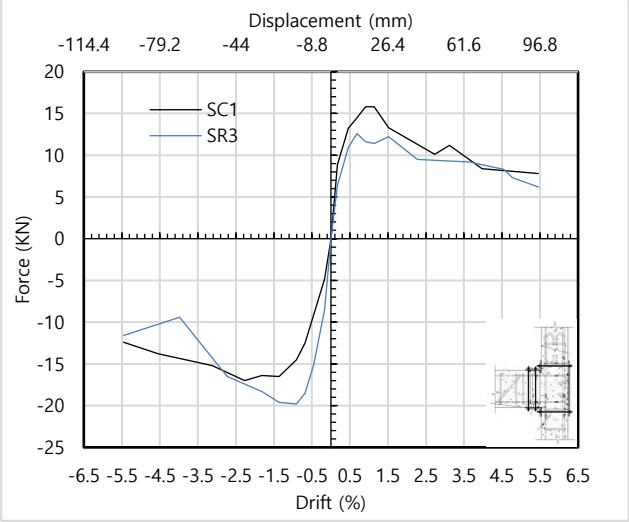

(a) Exterior beam-column joints

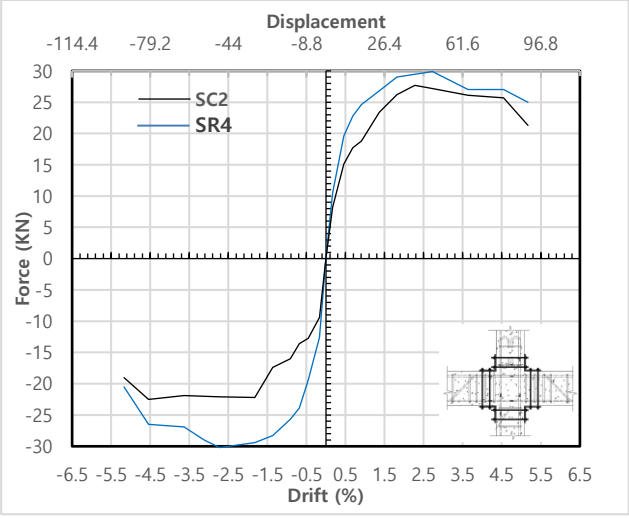

(b) Interior beam-column joints

Fig. 18 Comparison of force–displacement envelope curves of the control and retrofitted specimens

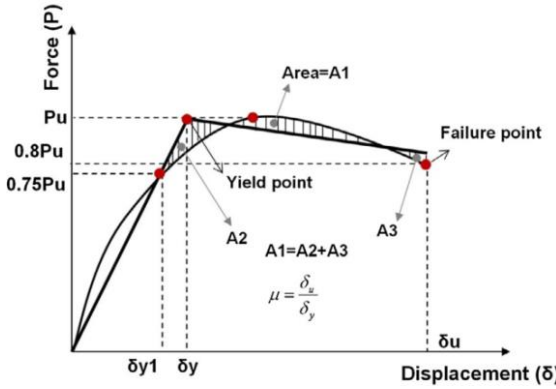

Fig. 19 Characteristic points on force-displacement curve

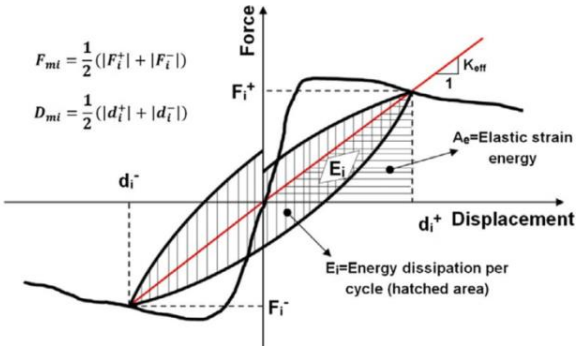

Fig. 20 Energy dissipation capacity and cyclic stiffness calculation

Table 5 shows that ductility ratio of Specimen SC1 represented an exterior beam-column joint is as high as 4.51 which is larger than expected. This may be justified by relatively large and stable slip of longitudinal reinforcements of the beams, and stability of the response is attributed to hooks at the end of the bars.

In Specimen SC2, representing an interior beam-column joint, the ratio of ductility was decreased to 3.82 which is 15% less than SC1, and this can be described by using continuous longitudinal bars and not having hooks at the end of bars in the beam. Table 5 indicates that specimens SR3 and SR4 representing two similar retrofitted exterior and interior beam-column joints, show increase of ductility ratios of 11% and 63%, relative to the control specimens SC1 and SC2, respectively.

Cyclic stiffness of the elements is estimated by the slope of the peak-to-peak line in each cycle of force-displacement hysteretic response (see Fig. 20). The first reversal cycle in each drift ratio is used to estimate the cyclic stiffness of the beam-column joint

$$K_i = \frac{F_i^+ - F_i^-}{d_i^+ - d_i^-} \quad (12)$$

Cyclic stiffness of both exterior and interior beam-column joints are shown in Fig. 21. The figure indicates relatively little difference between the retrofitted and the reference external joints over the entire range of deformations, i.e., before and after yield. But, Fig. 21(b) shows some 40% increase of stiffness for drifts less than 1% for interior retrofitted joint relative to the reference one.

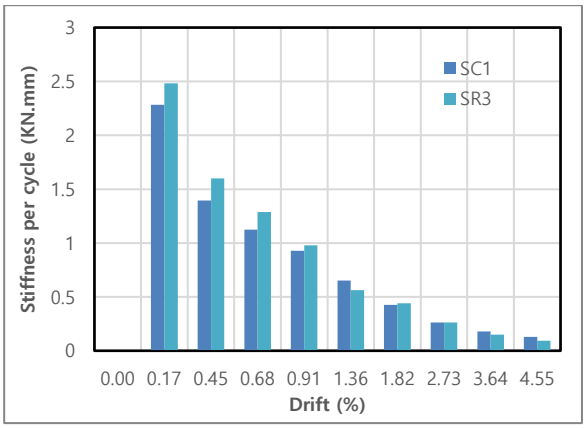

(a) Exterior beam-column joints

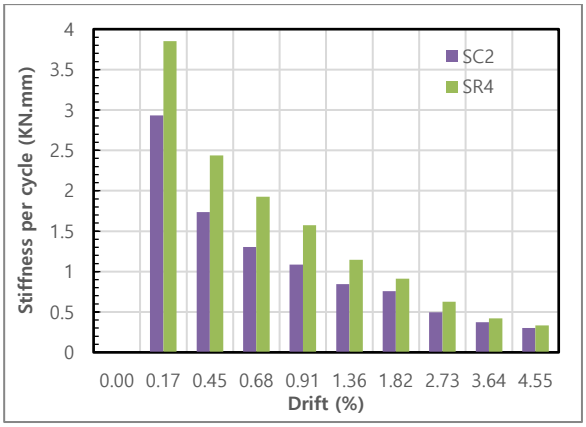

(b) Interior beam-column joints

Fig. 21 Comparison of stiffness per cycle up to 4.5% drift

Table 6 Comparison of seismic parameters for both control and retrofitted specimens

Specimen	Initial cyclic stiffness			Energy dissipation (drift 4.5%)			Nominal principal tensile stress		
	Control Spc	Retrofit Spc	Change	Control Spc	Retrofit Spc	Change	Control Spc	Retrofit Spc	Change
Exterior joint	2.28	2.48	+9%	10568	20520	+94%	$0.15\sqrt{f_c}$	$0.15\sqrt{f_c}$	+0%
Interior joint	2.93	3.85	+31%	10584	18690	+77%	$0.29\sqrt{f_c}$	$0.32\sqrt{f_c}$	+10%

However, this difference gradually diminishes when drift ratio exceeds 1%.

Other seismic parameters such as stiffness degradation, energy dissipation capacity, and nominal principal tensile stress for both control and retrofitted specimens are also presented in Table 6. It is seen that energy dissipation capacity of the retrofitted specimens is increased by 94% and 77% in comparison with control exterior and interior specimens, respectively; due to more confinement of joint panel zone in retrofitted specimens that has caused less slippage of bars in concrete throughout the joint. In addition, initial cyclic stiffness and nominal principal tensile stress of the retrofitted interior specimen has increased by 31% and 10%, respectively, in comparison with control specimen.

8. Damage index

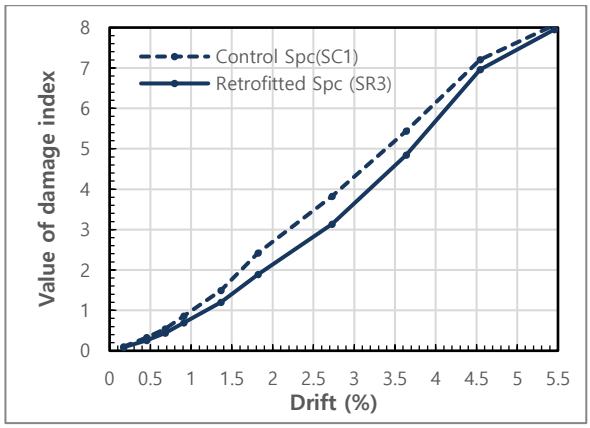

Fig. 22 Comparisons of the damage indices of control and retrofitted specimens

In the current study, the damage index of each specimen was evaluated using Park and Ang's damage model (Park and Ang 1985) as applied to RC beam-column joints by Karayannis *et al.* (2008). In this model, a linear combination of the damage caused by excessive deformations and the damage accumulated by the repeated cyclic loading effect are used

$$D = \frac{\delta_M}{\delta_u} + \frac{\beta}{Q_y.\delta_u}\int dE$$

where δ_M is the maximum displacement attained during seismic loading, δ_u is the ultimate displacement capacity under monotonic loading, β is a model parameter that depends on the value of shear force, axial force, and amount of longitudinal and confinement reinforcement, Q_y is the calculated yield strength, and dE is the incremental dissipated hysteretic energy. Values of δ_M, Q_y and dE are obtained from the experimental results of the joint specimens.

The ultimate displacement (δ_u) from tests was defined as the displacement at a predefined 20% drop below the maximum strength (Paulay and Priestley 1992). The model parameter β is taken to be 0.15 for retrofitted specimens as recommended by Cosenza *et al.* (1993) and to be 0.25 for the control specimens as recommended by Altoontash (2004). The calculated values of damage indices based on the above-described model are presented and compared in Fig. 22.

As shown in Fig. 22, the retrofitted specimen show a little less damage indices compared with the control specimen throughout the response. To the authors' opinion, this definition of damage index may not suit specimens reinforced by plain bars. This because of concentrated cracks in the specimens and lack of development of full capacity of the member strength relative to nominal sectional capacity of the specimens. In other words, failure of the specimens are strength control rather than energy control. Therefore, it may be more appropriate to define a new damage index or to make significant amendments to the above definition for plain bar specimens. It should be noted that, despite lack of improvement of damage index, the proposed retrofit method has successfully relocated the

large deformation zone to a distance away from the joint region (see Figs. 11 and 16).

9. Shear strength of exterior and interior joints without shear reinforcement

In previous studies (Pampanin *et al*. 2002, Calvi *et al*. 2002), the values of principal tensile stresses at first cracking has been reported as $f_t = 0.2\sqrt{f'_c}$ and $f_t = 0.29\sqrt{f'_c}$ for exterior joint (with end-hooks and smooth bars) and interior joint (with smooth bar), respectively. After first cracking, hardening behaviour develops until the tensile stress reaches $f_t = 0.42\sqrt{f'_c}$ for interior joints (Calvi *et al*. 2002).

Results of our tests show a value of $0.15\sqrt{f'_c}$ for principal tensile stress of exterior joint (see Fig. 23 and Table 7) by using Eqs. (1)-(11), which is less than the previous one ($f_t = 0.2\sqrt{f'_c}$) by 25%. It should be noted that in study by Calvi *et al*. (2002), the effect of axial load is not considered. In this study, two levels of axial loads are applied to two exterior joints: 7% and 15% of the section capacity ($A_g f'_c$). For specimen with higher axial load (Specimen SC1-1), as is expected, the principal tensile stress increases to $0.2\sqrt{f_c}$ (see Figs. 9 and 10(b)).

It is worth noting that the specimen with higher axial load, $0.15A_g f'_c$, did not undergo diagonal cracking at failure (see Fig. 9). In this specimen, sliding of plain bars causes deterioration of shear strength while axial load prevented shear cracks to appear.

For interior joints, results of our tests show a value of $0.3\sqrt{f'_c}$ for principal tensile stress (see Fig. 23 and Table 7) which is less than the previous one ($f_t = 0.42\sqrt{f'_c}$) by 28.5%. Regarding failure mode, diagonal cracking was not seen, again, and sliding of plain bars governed strength deterioration of the joint.

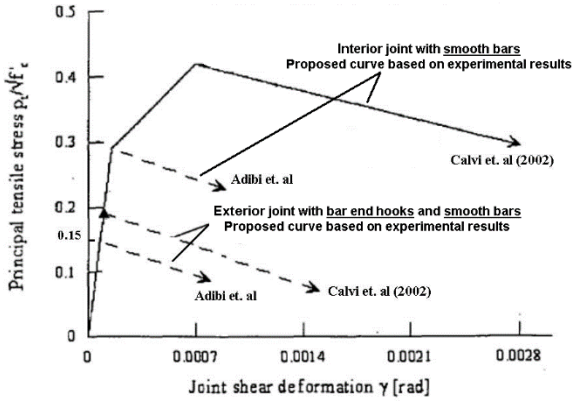

Fig. 23 Shear degradation models for external joints

Table 7 Values of different parameters of exterior and interior joints

Specimen		Peak load (KN)	M_b (kN.m)	T_2 (kN.m)	V'_c (kN)	F_a (MPa)	V_{jh} (MPa)	f_t (MPa)	Diagonal cracking
Exterior joint	SC1	15.8	25.93	97.9	15.8	1.61*	1.31	$0.15\sqrt{f_c}$	Observed
	SC1-1	23.8	39.05	147.4	39.1	3.22**	1.98	$0.2\sqrt{f_c}$	Not observed
Interior joint	SC2	27.69	20.76	78.4	27.7	1.61	2.07	$0.29\sqrt{f_c}$	Not observed

*: f_a=0.07 $A_g f'_c$
**: f_a=0.15 $A_g f'_c$

10. Conclusions

In this study, an enlargement technique to retrofit external and internal beam-column joints of old fashioned RC structures is examined. The technique uses external prestressed cross ties with steel angles and has already been used for substructures reinforced by deformed bars. It has advantages such as efficient enhancement of seismic capacity and lack of damage to the joint.

In our study, the technique has been applied to structures reinforced by plain bars. In concrete structures reinforced by plain bars, the behavior of joints is different from those reinfeorced by deformed bars. The test program includes cyclic load test of three reference specimens and two retrofitted specimens. The units are tested under increasing lateral cyclic load in combination with constant axial load. The tests show:

- A value of $0.15\sqrt{f'_c}$ for principal tensile stress of exterior joint which is less than the previously reported value ($f_t = 0.2\sqrt{f'_c}$) by 25%.

In this study, two levels of axial loads are applied to two exterior joints: 7% and 15% of the section capacity ($A_g f'_c$). For specimen with higher axial load (Specimen SC1-1),

- The principal tensile stress increases to $0.2\sqrt{f'_c}$,
- Sliding of plain bars causes deterioration of shear strength while axial load prevented shear cracks to appear.

For interior joints, the tests show:

- A value of $0.3\sqrt{f'_c}$ for principal tensile stress which is less than the previously reported value ($f_t = 0.42\sqrt{f'_c}$) by 28.5%.
- Regarding failure mode, diagonal cracking was not seen, again, and sliding of plain bars governed strength deterioration of the joint.

The retrofitted specimens show significant improvement in both ductility and relocation of the plastic joints far from the column face. The tests demonstrated a relatively large pinching in the hysteresis response of the control specimens. The pinching may be attributed primarily to sliding of the smooth bars. The retrofit method:

- Has increased ductility ratio of the interior beam-column joints by 63%, and energy dissipation capacity by 77%. relative to the control specimens,
- Has increased ductility ratio of the exterior beam-column by 11%, and energy dissipation capacity by 94% relative to the control specimens,
- Has successfully relocated the plastic joints into a place far from the column face inside the beam span.
- Has improved shear strength of the joints by less than 10%.

Overall, the proposed technique has successfully improved seismic capacity of the beam-column joints, even with minimum level of retrofit, that is, relatively small angle, and a rate of prestressing of 0.5 of the cross ties, with no stiffeners.

References

ACI 374.1-05 (2005), *Acceptance criteria for moment frames based on structural testing and commentary*, Farmington Hills, Michigan, USA.

ACI 374.2R-13 (2005), *Guide for testing reinforced concrete structural elements under slowly applied simulated seismic loads*, Farmington Hills, Michigan, USA.

Altoontash, A. (2004), "Simulation and damage models for performance assessment of reinforced concrete beam-column joints", Stanford University, Ph.D. Thesis.

ATC (1989), "Handbook for Seismic Evaluation of Existing Buildings ATC-22", Applied Technology Council, Redwood City, California.

Barker, J.A. (1979), *Reinforced Concrete Detailing*, Oxford University press, 2nd Edition, London.

Bedirhanoglu, I., Alper Ilki, Santiago Pujol and Nahit Kumbasar (2010), "Behavior of deficient joints with plain bars and low-strength concrete", *ACI Struct. J.*, **107**(3), 300.

Braga, F., Gigliotti, R. and Laterza, M. (2009), "R/C existing structures with smooth reinforcing bars: Experimental behaviour of beam-column joints subject to cyclic lateral loads", *Open Constr. Build. Technol. J.*, **3**, 52-67.

Braga, F., Gigliotti, R., Laterza, M., D'Amato, M. and Kunnath, S. (2012), "Modified steel bar model incorporating bond-slip for seismic assessment of concrete structures", *J. Struct. Eng.*, **138**(11), 1342-1350.

Calvi, G.M., Magenes, G. and Pampanin, S. (2002), "Relevance of beam-column joint damage and collapse in RC frame assessment", *J. Earthq. Eng.*, **6**(1), 75-100.

Cosenza, E., Manfredi, G. and Ramasco, R. (1993), "The use of damage functional in earthquake engineering, a comparison between different methods", *Earthq. Eng. Struct. Dyn. J.*, **22**(10), 855-868.

D'Amato, Braga, F., Gigliotti, R., Kunnath, S. and Laterza, M. (2012), "Validation of a Modified Steel Bar Model Incorporating Bond-Slip for Seismic Assessment of Concrete Structures", *J. Struct. Eng.*, **138**(11), 1351-1360.

Dimitrios, A. and Tsonos, G. (2010), "Performance enhancement of R/C building columns and beamcolumn joints through shotcrete jacketing", *Eng. Struct. J.*, **32**(3), 726-740.

Din 1045 (1959), *Bestimmungen fur die Ausf˙uhrung von Bauwerken aus Stahlbeton,* Deutscher Ausschuss für Stahlbeton, Berlin, Köln, Germany.

Duhman, C.W. (1953), *The Theory and Practice of Reinforced Concrete*, McGraw-Hill Book co.

Edvard, N.J. and Tanner, J.L. (1996), *Theory and problems of Reinforced Concrete Design*, Schaum Publishing co., USA

Guerrin, A. (1959), *Traite De Beton Arme,* Dunod, Paris.

Hakuto, S., Park, R. and Tanaka, H. (1999), "Effect of deterioration of bond of beam bars passing through interior beam-column joints on flexural strength and ductility", *ACI Struct. J.*, **96**(5), 858-864.

Hakuto, S., Park, R. and Tanaka, H. (2000), "Seismic Load Tests on Interior and Exterior beam-column Joints with Substandard Reinforcing Details", *ACI Struct. J.*, **97**(1), 11-25.

Karayannis, C.G., Chalioris, C.E. and Sirkelis, G.M. (2008), "Local retrofit of exterior RC beam-column joints using thin RC jackets", *J. Earthq. Eng. Struct. Dyn.*, **37**(5), 727-746.

Liu, A. and Park, R. (2000), "Seismic behavior of existing moment-resisting frames with plain round reinforcing bars designed to pre-1970s codes", *Proceeding of 12th world conference on earthquake engineering*, Auckland, New Zealand, February.

Liu, A. and Park, R. (2001), "Seismic behaviour and retrofit of pre 1970's as built exterior beam-column joint reinforced by plain bars", *Bull. NZ. Soc. Earthq. Eng.*, **34**(1), 68-81.

Manfredi, G., Verderame, G.M. and Lignola, G.P. (2008), "A F.E.M. model for the evaluation of the seismic behavior of interior joints in reinforced concrete frames", *Proceedings of the 14th World Conference on Earthquake Engineering*, Bejing, China, October.

Marthong, C., Deb, S.K. and Dutta, A. (2016), "Experimental fragility functions for exterior deficient RC beamcolumn connections before and after rehabilitation", *Earthq. Struct.*, **10**(6), 1291-1314.

Marthong, C., Dutta, A. and Deb, S.K. (2013), "Seismic rehabilitation of RC exterior beam-column connections using epoxy resin injection", *J. Earthq. Eng.*, **17**(3), 378-398.

Masi, A., Santarsiero, G., Verderame, G., Russo, G., Martinelli, E., Pauletta, M. and Cortesia, A. (2009), "Capacity models of beam-column joints: provisions of european and italian seismic codes and possible improvements", *Conference: Reluis Italian National Research Project*, Italy, April.

Pampanin, S., Calvi, G.M. and Moratti, M. (2002), "Seismic behaviour of R.C. beam-column joints designed for gravity loads", *Proceeding of 12th European Conference on Earthquake Engineering*, London, UK, September.

Pampanin, S., Christopoulos, C. and Chen, T.H. (2006), "Development and validation of a metallic haunch seismic retrofit system for existing under-designed RC frame buildings", *Earthq. Eng. Struct. Dyn.*, **35**(14), 1739-1766.

Parate, K. and Ratnesh Kumar (2016), "Investigation of shear strength models for exterior RC beam-column joint", *Earthq. Struct.*, **58**(3), 475-514

Park, R. (1989), "Evaluation of ductility of structures and structural assemblages from laboratory testing", *Bull. NZ. Soc. Earthq. Eng.*, **22**(3), 155-166.

Park, R. (2002), "A Summary of results of simulated seismic load tests on RC beam-column joints, beams and columns with substandard reinforcing details", *J. Earthq. Eng.*, **6**(2), 147-174.

Park, R., Billings, I.J., Clifton, G.C., Cousins, W.J., Filiatrault, A., Jennings, D.N., Jones, L.C.P., Perrin, N.D., Rooney, S.L., Sinclair, J., Spurr, D.D., Tanaka, H. and Walker, G. (1995), "The Hyogo-ken Nanbu Earthquake (The Great Hanshin Earthquake) of 17 January 1995", Report of the NZNSEE Reconnaissance Team, *Bull. NZ. Natl. Soc. Earthq. Eng.*, **28**(1), 1-98.

Park, Y. and Ang, A. (1985), "Mechanistic seismic damage model for reinforced-concrete", *Struct. Eng. J.*, ASCE, **111**(4), 722-739.

Paulay, T. and Priestley, M.J.N. (1992), *Seismic design of reinforced concrete and masonry buildings*, John Wiley & Sons, Inc, New York, NY, USA.

Pernot, P. (1954), *Le Beton Arme*, J. B. Balliere et Fils, Editeurs, Paris.

Pimanmas, A. and Chaimahawan, P. (2010), "Shear strength of beamcolumn joint with enlarged joint area", *Eng. Struct. J.*, **32**(9), 2529-2545.

Priestley, M.J.N. and Park, R. (1987) "Strength and ductility of concrete bridge columns under seismic loading", *ACI Struct. J.*, **84**(1), 61-76.

Röhma, C., Novák, B., Sasmal, S., Karusala, R. and Srinivas, V. (2012), "Behaviour of fibre reinforced beam-column sub-assemblages under reversed cyclic loading", *Constr. Build. Mater. J.*, **36**, 319-329

Russo, G. and Margherita Pauletta (2012), "Seismic behavior of

exterior beam-column connections with plain bars and effects of upgrade", *ACI Struct. J.*, **109**(2), 225

Sezen, H., Elwood, K.J., Whittaker, A.S., Mosalam, K.M., Wallace, J.W. and Stanton, J.F. (2000), "Structural Engineering Reconnaissance of the August 17, 1999 Kocaeli (Izmit), Turkey Earthquake", Technical Rep. No., PEER 2000, 9.

Sezen, H., Whittaker, A.S., Elwood, K.J. and Mosalam, K.M. (2003), "Performance of reinforced concrete buildings during the August 17, 1999 Kocaeli, Turkey earthquake, and seismic design and construction practice in Turkey", *Eng. Struct. J.*, **25**(1), 103-114.

Shafaei, J., Hosseini, A. and Marefat, M. (2014a), "Seismic retrofit of exterior RC beam-column joints by joint enlargement using prestressed steel angles", *Eng. Struct. J.*, **81**, 265-288.

Shafaei, J., Zareian, M., Hosseini, A. and Marefat, M. (2014b), "Effects of joint flexibility on lateral response of reinforced concrete frames", *Eng. Struct. J.*, **81**, 412-431.

Shigeru, H. (1995), Retrofitting of reinforced concrete moment Resisting Frames. research report Dept. Civil. Engineering, Univ. of Canterbury, NZ (supervised by R. Park and H. Tanaka) ISSN0110-3326.

Soleimani, D., Popov, E.P. and Bertero, V.V. (1979), "Hysteretic beahavior of reinforced concrete beamcolumn subassemblages", *ACI J.*, **76**(11), 1179-1195.

CC